H-mode density limit studies at ASDEX Upgrade

M. Bernert, A. Kallenbach, T. Eich, T. Happel, P.T. Lang, S. Potzel, F. Reimold,
J. Schweinzer, B. Sieglin, E. Viezzer and the ASDEX Upgrade team
Max Planck Institute for Plasma Physics, EURATOM Association, 85748 Garching, Germany

Introduction

The H-mode regime is the operational scenario foreseen for ITER, DEMO and future fusion power plants based on the tokamak design. It is favorable to operate a fusion power plant at high density to maximize its fusion power. However, the achievable H-mode density in tokamaks is limited by a back transition to L-mode, which occurs at line-averaged densities corresponding to Greenwald fractions of about 0.8-1 [1]. This fraction is given by the density normalized to the Greenwald limit ($n_{GW} \propto \frac{I_p}{\pi a}$), which is empirically found for L-mode operation. This H-mode density limit (HDL) has been investigated for ASDEX Upgrade (AUG) with the full tungsten wall.

Experiments

Several density ramp discharges were carried out at AUG in order to study the HDL. This set of 29 discharges includes dedicated scans of several operational parameters, such as plasma current ($I_P = 0.4-1.0\,\text{MA}$), safety factor ($q_{95} = 3.5-6$) and external heating power ($P_{heat} = 5-12.5\,\text{MW}$). In order to reach the HDL, the pumping capacity of the experiment was reduced by turning off the cryo pump. By this measure the required neutral pressures of up to 6 Pa in the divertor could be achieved.

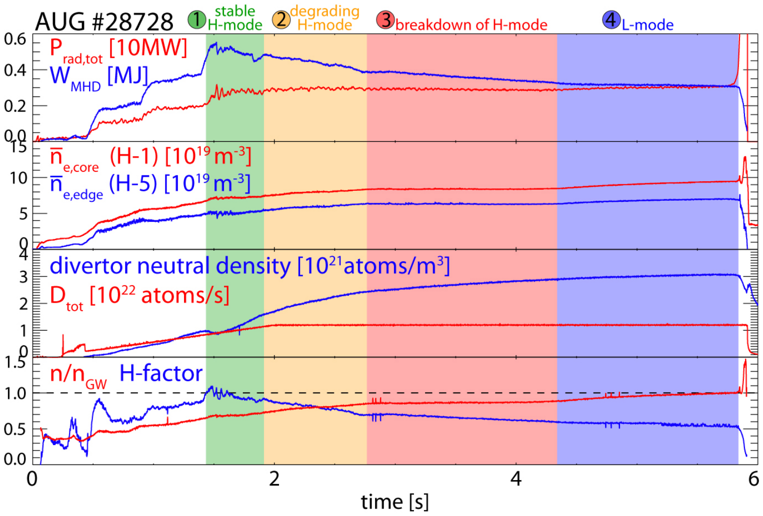

Figure 1: Overview of the main parameters of a HDL discharge

An overview of the main parameters of a HDL discharge is shown in Fig. 1. While the neutral pressure increases, the line integrated density changes only slightly (fueling limit). Meanwhile, the plasma stored energy decreases monotonically. At the end, the discharge reaches the L-mode density limit and disrupts.

The four phases of the H-mode density limit

Each discharge can be separated into four phases indicated by the background colors in Fig. 1. These phases are identified by the temporal change of the density and the stored energy of the plasma.

The four distinct phases become clear when the pedestal top temperature or the plasma stored energy are plotted versus the edge line integrated density (Fig. 2). The phases are identified as (green) a stable H-mode, (orange) a degrading H-mode, (red) the breakdown of the H-mode and, finally, (blue) an L-mode phase. These four phases are reproduced in every HDL discharge,

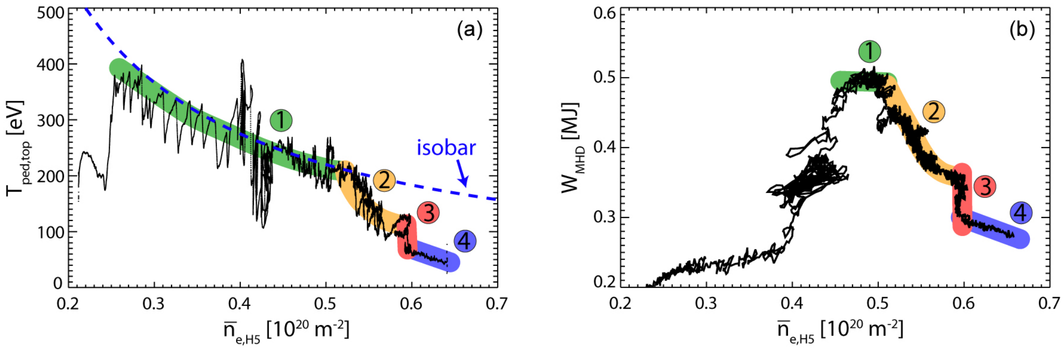

Figure 2: Estimate of pedestal top temperature (a) and plasma stored energy (b) plotted versus edge line integrated electron density for AUG #26902

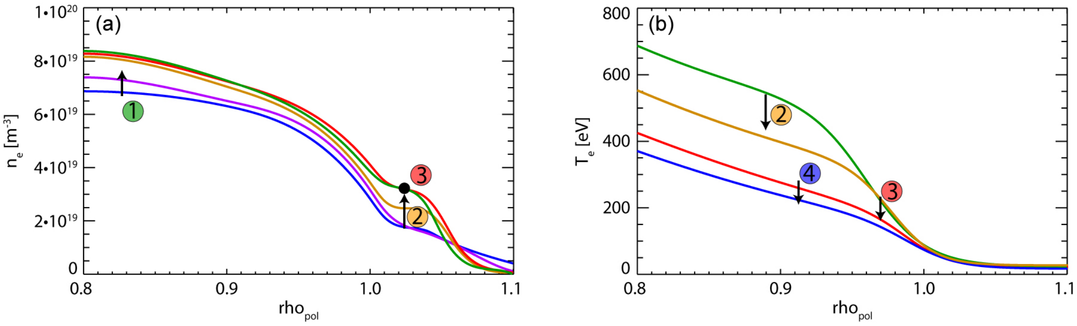

Figure 3: Evolution of electron density (a, AUG #28726) and temperature profiles (b, AUG #29809). Profiles cannot be provided for all phases. The arrows and numbers indicate the radial position and the phase in which the predominant changes in the profiles occur.

though the first phase might only be seen during the ramp up. The individual phases recover after changes or trips of the external heating, therefore, they are considered to be stable operational regimes of high density H-modes. The evolution of the electron density and temperature profiles can also be distinguished according to these phases (Fig. 3).

① During the stable H-mode phase, the stored energy and the confinement stay constant, while the density is increasing in the core. The temperature decreases inversely. The relationship between n_e and T_e evolves along an isobaric line towards higher densities (indicated in Fig. 2(a)). A transition from type I to type III edge localized modes (ELMs) takes place in this phase. Afterwards, the ELM frequency rises continuously and the relative ELM loss energy decreases. Fluctuations, which are most likely correlated with the detachment state [2], start to appear around the X-point and might be a sign for increased transport.

② During the degrading H-mode phase, the density increases marginally and the stored energy decreases. In Fig. 2 this is seen as a movement away from the isobaric line towards lower pressure, leading to a knee in the graph. In Fig. 3 one can see that the core density is fixed, while a plateau of electron density builds up in the scrape-off layer (SOL), which rises up to about half of the pedestal top density. The temperature pedestal width appears to become smaller, keeping the gradient constant at the separatrix. Accordingly, the pedestal top temperature decreases. Due to the profile stiffness also the core temperature decreases, leading to the reduced confinement and stored energy. The duration of this phase varies between the discharges in the database from 0.5 s to over 3 s.

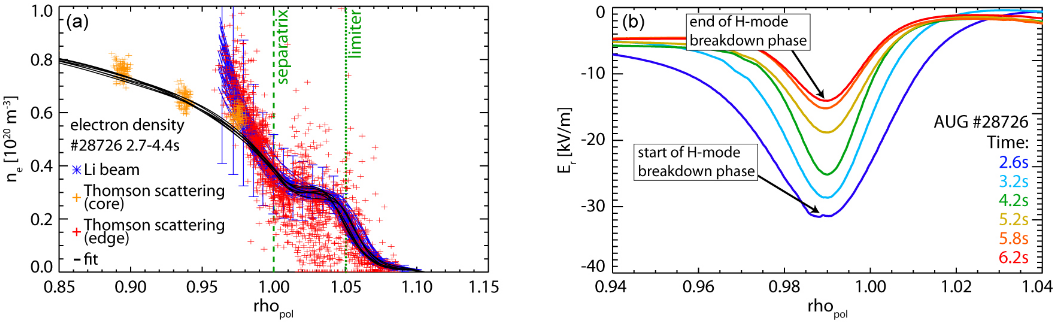

Figure 4: Evolution of electron density (a) and E_r (b, evaluated by $\frac{\nabla p_e}{n_e}$ [6]) in the third phase.

③ The breakdown phase of the H-mode is characterized by a sharp drop of the stored energy at a constant density profile, through the SOL, pedestal and core region. The constant density profile is shown in more detail in Fig. 4(a). The temperature pedestal vanishes, i.e. the pedestal gradient reduces. During this phase the ELMs vanish. However, electron temperature and radial electric field (E_r, Fig. 4(b)) are still at typical H-mode values during the whole phase. The duration of this phase varies between 0.1 s and 4 s within this set of discharges.

④ Eventually, in the L-mode phase, the density increases again and the stored energy decreases only slightly. The temperature decreases accordingly. It appears that the L-mode phase starts when the depth of the E_r well reaches the threshold value of about -15 kV/m [7], though there are considerable uncertainties in the evaluation. The detachment of the outer divertor evolves during this phase. The detachment is followed by a MARFE at the X-point, which initiates the disruption.

Comparison to proposed mechanisms of the H-mode density limit

In Ref. [3, 4], the full detachment of the outer divertor and MARFE formation were reported to cause the HDL in AUG with carbon walls. However, for the full-W AUG, detachment of the outer divertor and MARFE develop just during the L-mode phase. The different observations are the result of to the different wall materials and the resulting composition of the edge plasma. Furthermore, the total radiated energy is constant for the full-W AUG during all four phases (except the disruption). The poloidal radiation distribution and the power flux onto the divertor target plates change only marginally. Therefore, processes that lead to additional radiation losses, most prominently detachment and MARFEs, are not the main driver of the HDL.

In Ref. [1, 5], ELMs were discussed as potential triggers for the HDL. If the recovery time of the pedestal gradients were longer than the ELM cycle time, the pedestal would continuously be eroded. However, in several discharges the degradation of the confinement is ongoing (third phase) even though ELMs no longer appear. Thus, there must be another effect leading to the degradation.

In Ref. [7], a threshold of the depth of the E_r well of -15 kV/m is reported for the L- to H-mode transition. It is worth checking if a similar threshold is present at the back transition of the HDL. The E_r well depth at the beginning of the third phase varies between -25 and -35 kV/m for the various discharges in the database, and is hence well above the reported threshold. However, estimates of E_r indicate that the depth of the E_r well is close to -15 kV/m at the beginning of the L-mode phase (Fig. 4(b)). Thus, E_r does not trigger the HDL, but might be the reason for the final transition into L-mode.

Discussion

The observations of the four phases reveal that an additional energy loss channel must be present at the highest density H-modes (2nd and 3rd phase). This loss channel, which is most likely increased transport, erodes the E_r well depth and finally leads to the transition to L-mode. Along with the observed energy degradation, the fueling of the plasma changes. The combination of these two effects creates the four quasi-stable plasma regimes. However, both effects might be independent of each other, although both take place at high densities.

The fueling limit might be responsible for the density evolution. The fueling limit is not understood yet but might be caused by an outward shift of the ionization profile of recycling neutrals from the first wall. The density in the confined region would saturate and the ionization would take place mainly in the SOL. This is in agreement with the observed density plateau in the SOL. The increased density in the SOL or the shifted ionization profile might also be responsible for the additional energy loss channel. Possible candidates are increased charge exchange collisions with neutrals at the edge or increased transport by additional instabilities. Both effects could not be measured and further analysis is ongoing.

Exceeding the limit: Peaked density profiles

If the HDL and the Greenwald limit are edge determined limits, it should be possible to increase the core density and exceed the line averaged densities of these limits. However, the density profiles of the discharges in our database are flat due to the high collisionality ($\nu_{eff} > 1$).

Fig. 5 compares the density profiles of the highest density HDL discharge and a pellet fueled H-mode [8]. Due to the central fueling of the pellets, the core density does exceed the Greenwald density by about a factor of 2. The SOL density is almost unchanged and the energy confinement time stays about constant. Thus, it is possible to exceed the Greenwald limit and HDL with peaked density profiles, proving both to be edge limits.

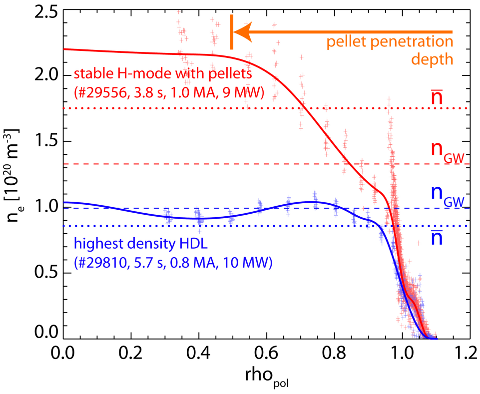

Figure 5: Density profiles of a stable pellet fueled H-mode and the highest density achieved of a purely gas puffed HDL discharge

Peaked density profiles are also intrinsically obtained at lower collisionalities ($\nu_{eff} \approx 0.5$)[9]. ITER, DEMO and future fusion power plants will operate at a lower collisionality and, therefore, are expected to have inherently peaked density profiles [10]. Following our work, it is likely, that these tokamaks operate in a stable H-mode regime at Greenwald fractions above 1.

References

[1] M. Greenwald, Plasma Phys. Control. Fusion **44**, R27 (2002)
[2] S. Potzel et al, J. Nucl. Mat., **438**, 285-290 (2013)
[3] K. Borrass et al, Contr. to Plasma Phys. **38**, 130 (1998)
[4] K. Borrass et al, Nucl. Fusion **44**, 752 (2004)
[5] K. Borrass et al, Nucl. Fusion **37**, 523 (1997)
[6] E. Viezzer et al, Nucl. Fusion **53**, 053005 (2013)
[7] P. Sauter et al, Nucl. Fusion **52**, 012001 (2012)
[8] P.T. Lang et al, Nucl. Fusion **52**, 023017 (2012)
[9] C. Angioni et al, Phys. Rev. Lett. **107**, 215003 (2011)
[10] C. Angioni et al, Plasma Phys. Control. Fusion **51**, 124017 (2009)